Novel Keplerate type polyoxometalate-surfactant-graphene hybrids as advanced electrode materials for supercapacitors

Dawid Pakulski, Adam Gorczyński, Wlodzimierz Czepa, Zhaoyang Liu, Luca Ortolani, Vittorio Morandi, Violetta Patroniak, Artur Ciesielski, Paolo Samorì

▶ **To cite this version:**

Dawid Pakulski, Adam Gorczyński, Wlodzimierz Czepa, Zhaoyang Liu, Luca Ortolani, et al.. Novel Keplerate type polyoxometalate-surfactant-graphene hybrids as advanced electrode materials for supercapacitors. Energy Storage Materials, 2018, 17, pp.186-193. 10.1016/j.ensm.2018.11.012 . hal-02058348

HAL Id: hal-02058348
https://hal.science/hal-02058348

Submitted on 5 Mar 2019

HAL is a multi-disciplinary open access archive for the deposit and dissemination of scientific research documents, whether they are published or not. The documents may come from teaching and research institutions in France or abroad, or from public or private research centers.

L'archive ouverte pluridisciplinaire **HAL**, est destinée au dépôt et à la diffusion de documents scientifiques de niveau recherche, publiés ou non, émanant des établissements d'enseignement et de recherche français ou étrangers, des laboratoires publics ou privés.

Novel Keplerate type polyoxometalate-surfactant-graphene hybrids as advanced electrode materials for supercapacitors

Dawid Pakulski,[a,b,c] Adam Gorczyński,[b] Włodzimierz Czepa,[b,c] Zhaoyang Liu,[a] Luca Ortolani,[d] Vittorio Morandi,[d] Violetta Patroniak,[b] Artur Ciesielski,[a,c]* Paolo Samorì[a]*

[a] Université de Strasbourg, CNRS, ISIS, 8 alleé Gaspard Monge, 67000 Strasbourg, France

E-mail : ciesielski@unistra.fr, samori@unistra.fr

[b] Faculty of Chemistry, Adam Mickiewicz University, Umultowska 89b, 61-614 Poznań, Poland.

[c] Centre for Advanced Technologies, Adam Mickiewicz University, Umultowska 89c, 61614 Poznań, Poland.

[d] CNR-IMM Bologna, via Gobetti 101, 40129 Bologna, Italy

Abstract

The development of novel materials for enhanced electrochemical energy storage applications, in particular for the fabrication of supercapacitors (SCs) displaying increased properties, is a milestone of both fundamental and technological relevance. Among nanostructured materials, polyoxometalates (POMs) combined with various carbon-based nanostructures represent a very promising class of hybrid systems for energy storage, yet, guidelines for their rational design and synthesis leading to high-performance SCs is still lacking. Here, we have produced a novel hybrid architecture based on Keplerate type POM (Mo_{132}) functionalized with dodecyltrimethylammonium bromide (DTAB), which upon mixing with electrochemically exfoliated graphene (EEG) nanosheets results in the formation of porous 3D superstructures. Mo_{132}-DTAB-EEG combines the redox activity of POMs and high electrical conductivity of graphene, all synergically mediated by the surfactant-assisted porosity enhancement, to form new electrode materials for SCs. Cyclic voltammetry and galvanostatic charge/discharge electrochemical studies on Mo_{132}-DTAB-EEG performed in aqueous H_2SO_4 electrolyte revealed that the unique combination of these three components yields highly efficient energy storage materials. In particular, our highly porous hybrids system exhibits high specific capacitance of 65 F g^{-1} (93 F cm^{-3}, 93 mF cm^{-2}) combined with excellent stability (99% of specific capacitance retained) after 5000 charge/discharge cycles at different current densities, overall displaying

significantly improved performance compared to pristine electrochemically exfoliated graphene material. Strong non-covalent interactions between Keplerate type polyoxometalate Mo_{132}-DTAB and graphene surface offer higher stability compared to other hybrid POM/carbon-based systems, and unique electrical properties of the multicomponent structure, thereby paving the way towards the development of novel, and potentially multifunctional, POM-based architectures to be exploited as SC electrode materials.

Keywords

Electrochemically Exfoliated Graphene, Polyoxometalate, Keplerate, Inorganic-Organic Hybrids, Surfactant Encapsulated Clusters (SEC), Supercapacitor.

1.Introduction

The search for technological solutions to the ever-increasing demand in energy consumption represents one of the greatest challenges our society is facing nowadays. Sustainable energy-management *via* optimized energy generation and storage are two strategies which have been identified as potential solution to this colossal problem [1]. The tremendous pace towards miniaturized electronics calls for the development of increasingly smaller and lighter energy-storage components that can enable autonomous and sustained operation of electronic devices for applications such as wearable electronics and portable sensors [2]. (Micro)supercapacitors, which provide higher power and longer life-cycle of (micro)batteries, have been identified as a viable route for this purpose, because, despite they can store less energy than batteries, they can be charged and discharged much more rapidly and have an almost unlimited lifetime [3]. Specifically, supercapacitors (SCs) and electrochemical capacitors are being recognized as a new generation of energy storage devices [4, 5] since they outperform batteries due to power density, higher stability and the overall improved safety tolerance [6-10].

A plethora of different systems have been proposed as electrode materials for SCs aiming at increasing their capacitance and energy density, to ultimately leverage the energy storage capacity. The performance of the SC can be enhanced by exploiting two different processes: (i) the electric double-layer (EDL) mechanism, and (ii) the pseudocapacitance. In former, the generation of sub-nanometer sized EDL between ions and the negatively charged electrode is responsible for the energy storage [6]. Here, different forms of (nano)carbon species [11-19] (*e.g.* activated and porous carbon, carbon nanotubes, and recently graphene) have been primarily used due to their high electrical conductivities and wide availability, accompanied by their finely tunable morphologies. In the latter, the energy storage processes result from the reversible surface redox reactions which occur at the interface between the electrode and the electrolyte [20]. Such pseudocapacitive contributions are mostly found in transition metal oxides or chalcogenides (*e.g.* RuO_2 [21], MoS_2 [22]), conducting polymers (*e.g.* polyaniline [23], polypyrrole [24], polyethylenimine [25]) and carbon materials functionalized with nitrogen/oxygen moieties [4]. However, if taken individually each SC component suffers from certain disadvantages that preclude their viable implementation into the next generation of supercapacitive devices [9]. For example, active carbon materials display wide pore size distribution and limited charge storage capability, whereas metal oxides exhibit low electronic conductivity. A practical way to overcome such limitations consists in combining two or more of the above components into hybrid material and thus synergically combine both the EDL and the pseudocapacitive energy storage mechanisms to form enhanced SCs.

Polyoxometalates (POMs) [26, 27] can be regarded as well-defined, larger analogues of metal oxide clusters [28] exhibiting rich redox characteristics [29], thus appearing as ideal candidates to achieve enhanced pseudacapacitive behaviour in SCs. In particular, POMs can exhibit Faradaic charge-storage properties without loss of their robust architecture and do not hamper the EDL capacitive storage mechanisms coming from the conductive support[28].Indeed, POMs, in the form of $H_3PMo_{12}O_{40}$, was first used for electrochemical capacitors in 1998 [30]. Later, in 2005 [31], a major improvement was achieved by exploiting hybrid POM/PA (with POM being $H_4SiW_{12}O_{40}$, $H_3PW_{12}O_{40}$ or $H_3PMo_{12}O_{40}$, and PA being polyaniline). The high solubility of POMs in aqueous solutions can be circumvented by its deposition on carbon supports such as (MW)CNT [32-37], activated carbon (AC) [38-40] and various forms of graphene [41-47], simultaneously taking advantage of their outstanding electronic properties. These particularly appealing classes of hybrids are yet to be thoroughly explored, as they hold great potential for technological applications in catalysis, sensing and electronics [48-51].

In order to enhance the device performance, including energy capacity, power density and recharge time, the ability to effectively control the electrodes nanostructure is essential [3]. Such a control can be achieved in POM based surfactant encapsulated clusters [52]. Noteworthy, although over 10 different topological types of POM architectures can be designed [53], to date research on their application as SC materials was limited to the prototypical Wells-Dawson and Keggin building blocks [29, 38]. While polyoxometalates may act as electron acceptors/donors to accelerate electron transfer and improve the overall conductivity of hybrid structures, their interaction with carbon-based materials is relatively weak, ultimately affecting the stability of the POM-based hybrid structures. To overcome this issue, herein we introduce for the first time the use of the Keplerate type polyoxometalate Mo_{132}, i.e. POM bearing 42 negative charges on its outer-sphere surface, that can be easily functionalized with a surfactant exposing long alkyl chains. Such molecules are known to possess a high adsorption energy on carbon-based surfaces which can be key towards the generation of stable, graphene-supported electroactive material for supercapacitors. The use of a facile, two-step synthetic methodology relying on surfactant-encapsulation [54, 55] made it possible to synthesize Mo_{132}-DTAB cluster (with Mo_{132}being$(NH_4)_{42}[Mo^{VI}_{72}Mo^{V}_{60}O_{372}(CH_3COO)_{30}(H_2O)_{72}]$ and DTAB consisting of dodecyltrimethylammonium bromide). Such hybrid system upon combination with the electrochemically exfoliated graphene (EEG) forms novel porous hybrid Mo_{132}-DTAB-EEG. Enhanced supercapacitive performances of the Mo_{132}-DTAB-EEG compared to EEG were recorded, which can be ascribed to higher porous nature of the novel POM based composite in combination with its excellent electrochemical stability when subjected to cycling in acidic

aqueous environment (1M H_2SO_4). Thus, a simple and efficient methodology is provided that relies on two energy storage mechanisms, EDL originated from EEG and pseudocapacitance resulting from Mo_{132}, synergically mediated by the DTAB surfactant.

2. Experimental methods

2.1 Preparation of electrochemically exfoliated graphene (EEG)

Graphene was prepared by making use of the well-established electrochemical exfoliation (EEG) by exploiting graphite foil as anode and a platinum wire as the counter electrode [56]. Both elements of the electrolytic cell were soaked in aqueous solution of 0.1 M $(NH_4)_2SO_4$. The working electrode's exfoliation occurs as an immediate consequence of the applied voltage between the two electrodes, for example, +15 V (ISO-TECH IPS-603 DC power supply), which generates a starting current of ~0.4 A. The exfoliation was running for ca. three hours, i.e. until the graphite foil was completely exfoliated. The obtained material was then rinsed several times with ethanol in order to remove salt residuals and filtrated using PTFE membranes (pores diameter of 5 μm). Finally, the collected material was dispersed in DMF by mild sonication for 30 min. Such dispersion was followed by a 48 hours lasting decantation in order to promote the sedimentation of unexfoliated graphite.

2.2 Preparation of surfactant encapsulated polyoxometalate Mo_{132}-DTAB

Keplerate type polyoxometalate Mo_{132} was synthesized according to the procedure previously reported by Müller and co-workers [57]. The preparation of the POM-surfactant (Mo_{132}-DTAB) hybrid material was carried out by exploiting the methodology previously described [58] (see *supporting information* for more details). The obtained complex (Mo_{132}-DTAB) has a chemical formula of $(CH_3(CH_2)_{11}N(CH_3)_3)_{40}(NH_4)_2[Mo_{132}O_{372}(CH_3COO)_{30}(H_2O)_{72}]$ x $40H_2O$ as determined by elemental analysis [59].

2.3 Preparation of hybrid inorganic-organic modified graphene material Mo_{132}-DTAB-EEG

To graft the Mo_{132}-DTAB molecules onto the surface of graphene (EEG), an acetone solution on Mo_{132}-DTAB was added to DMF suspension of EEG under vigorous stirring at the room temperature for 12 hours. Finally, the precipitate was isolated by filtration, washed several times using acetone and ethanol and dried in air (see SI for more details).

2.4 Preparation of supercapacitor electrodes

The supercapacitor working electrode was fabricated by mixing 80 wt% Mo_{132}-DTAB-EEG, 10 wt% carbon black and 10 wt% poly(tetrafluoroethylene) binder dispersed in water. After sufficient grinding the mixture in ethanol, the obtained paste was pressed onto a platinum mesh which served as current collector, followed by drying in a vacuum oven for 6 hours.

2.5 Electrochemical measurements

Electrochemical measurements, including cyclic voltammetry, were performed with a PGSTAT204 instrument (Autolab). The electrochemical capacitive of Mo_{132}-DTAB-EEG was evaluated in a three-electrode system, applying 1 M H_2SO_4 as electrolyte, platinum plate and Ag/AgCl (saturated KCl) as the counter and reference electrodes, respectively. The scan rates varied from 1 mV/s to 100 mV/s. The specific capacitance is normalized by the weight of Mo_{132}-DTAB-EEG. The stability tests were performed at 100 mV/s for 5000 cycles. All electrochemical experiments were carried out at room temperature.

2.6 Materials characterizations

All chemicals and solvents were purchased from commercial sources (mainly Sigma-Aldrich) and used without further purification.

Scanning (SEM) and transmission electron microscopy (TEM) characterizations were carried out by using a SEM FEI Quanta 250 FEG instrument with energy-dispersive X-ray (EDX) and FEI Tecnai F20 S/TEM equipped with EDX. Thermogravimetric analysis (TGA) was performed on a Mettler Toledo STAR System TGA/DSC 2 set-up operating with a heating rate of 10 °C min^{-1} under flowing air. The Fourier transform infrared spectra (FT-IR) were recorded within the mid-IR range (400−4000 cm^{-1}) by using a Spectrum Two FT-IR spectrometer (Perkin Elmer) equipped with ATR Diamond. X-ray photoelectron spectroscopy (XPS) analyses were done by employing a Thermo Scientific KAlpha X-ray photoelectron spectrometer with a basic chamber pressure of ~10^{-9} mbar and an Al anode as the X-ray source (X-ray radiation of 1486 eV). Spot sizes of 400 µm were used and pass energies of 200.00 eV for wide energy scans, while for normal scans 10.00-20.00 eV were used. Organic elemental analysis (C, H, N) was done by following standard procedure using Thermo Scientific FLASH 2000 HT/IRMS Analyzers. Hydrodynamic radius analyses were executed using Malvern Zetasizer Nano S instrument, equipped with a 630 nm He-Ne laser, with the detector collecting the backscattering signal (173° geometry). The specific surface areas were measured by means of a Micromeritics ASAP 2050 surface area and porosity analyzer. Prior to the BET

measurements, the samples were degassed for 10 hours at 100 °C. Adsorption isotherms were calculated for nitrogen adsorption at 77 K and pressures up to 1 bar. X-ray powder diffraction (XRD)was performed on a Bruker ASX D8 Advanced equipped with Cu anode with Kα radiation (λ = 1.5418 Å). Diffraction patterns were collected at room temperature in the scattered angular range between 6° and 60° with an angular resolution of 0.02° per step and a typical counting time 4 of 10 s per step.

3. Results and discussion

Mo_{132} is a POM nanocapsule displaying an icosahedral symmetry and comprising over 500 atoms, being arguably one of the largest spherical POM ever produced [60]. Since its first successful synthesis by Müller [57] this building block attracted a great interest because of its structural and catalytic properties [61, 62]. Hitherto, only one article reported on the use of Mo_{132} as composite component in metal oxide semiconductor photoelectrodes [63]. This is surprising, especially given that the redox electronic properties of Mo_{132} and its inherent porous structure are key characteristics which makes it ideal component for the generation of efficient SC devices. This prompted us to focus on this species to construct novel, electronically active hybrid materials and ultimately prove that the Keplerate clusters are promising class of POMs that are worth further studies towards energy applications.

Size of Mo_{132} POM allows one to utilize its inorganic core for the effective formation of large surfactant-encapsulated clusters (SECs), effectively leading to decoration of POM with notable number of surfactant molecules. We have thus demonstrated herein a facile protocol for the fabrication of Mo_{132}-DTAB-EEG hybrid system as schematically illustrated in Fig. 1, with dodecyltrimethylammonium bromide (DTAB) as the surfactant of choice.

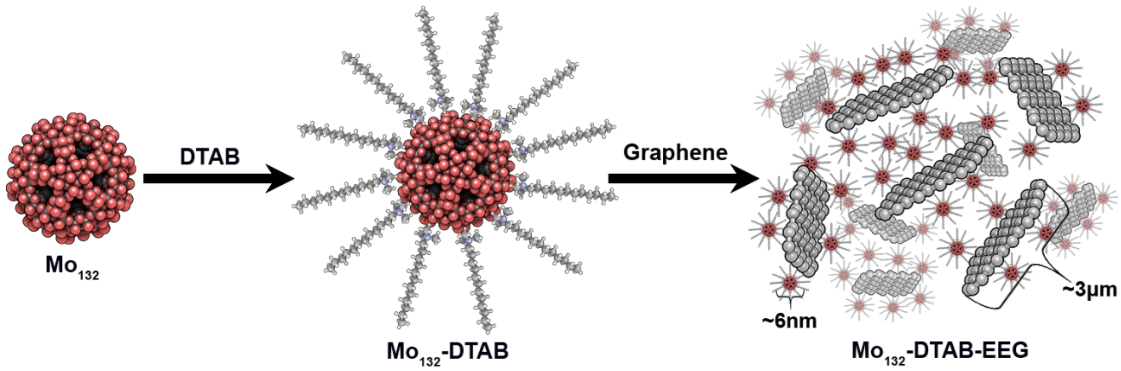

Fig. 1. Schematic representation of the formation of **Mo_{132}-DTAB-EEG** hybrid material.

The role of the DTAB surfactant is crucial in the process of Mo132-DTAB-G formation, since DTAB molecules not only increase the strength of van der Waals interactions between the Mo132 and electrochemically exfoliated graphene, but also results in synergically increased porosity of the Mo132-DTAB-EEG and thus enhanced supercapacitive performance of the hybrid material. In theory it should be possible to screen a variety of different surfactants (surfs) to form a relevant family of Mo132-surf-EEG hybrids, though it would be difficult to pre-determine which surfactant would be the most suitable for the electrochemical applications. Noteworthy, the influence of the surfactant on the morphology of obtained surfactant encapsulated clusters (SECs) is known phenomenon and could result in the synthesis of assemblies of different porosity, or even preclude the formation of SECs *per se* [52]. We have performed such preliminary studies by using four different surfactants, i.e. DTAB- dodecyltrimethylammonium bromide, DDAB - didodecyldimethylammonium bromide, DODA- dioctadecyldimethylammonium bromide, TODA - octadecyltrimethylammonium bromide, accounting for different number and length of employed organic chains. Certain synthetic problems were encountered that concern the phase purity and homogeneity of synthesized species with DDAB and DODA as the surfactant, which resulted in successful formation of two hybrids materials with one alkyl chain (Mo_{132}-DTAB-EEG, Mo_{132}-TODA-EEG). Initial electrochemical tests showed that Mo_{132}-DTAB-EEG is far superior material than Mo_{132}-TODA-EEG, therefore the former one was used for further research.

Mo_{132}-DTAB-EEG hybrid material can be efficiently generated by exploiting a self-assembly protocol which relies on two different types of non-covalent interaction: (i) Mo_{132}-DTAB system can be formed by using electrostatic interactions holding together the Keplerate POM Mo_{132} and the DTAB surfactant, and (ii) the grafting of Mo_{132}-DTAB onto the electrochemically exfoliated graphene nanosheets (EEG) via van der Waals type interactions. Noteworthy, the use of one-pot reaction, with all three components mixed together simultaneously, led to disordered structures; therefore, a two-step synthesis has been employed to guarantee homogenous dispersion of the component in the hybrid structure.

3.1 Synthesis and characterization

Both the Keplerate type polyoxometalate (Mo_{132}) and polyoxometalate functionalized with surfactants (Mo_{132}-DTAB) were synthesized according to the procedures reported by Müller and co-workers [57, 64]. The hydrophobic DTAB surfactant was used to decorate a highly hydrophilic Mo_{132} POM, both structural components bound *via* strong electrostatic interactions.

Mo_{132}-DTAB adopts a spherical morphology (see Fig. S3), which also indicate that a 'lipophilic layer' of DTAB molecules decorates the POMs surface – a final result being a brown solid of Mo_{132}-DTAB compound that is well soluble in organic solvents but insoluble in water. The structure and the chemical composition of the obtained product was confirmed by routine analytical methods (FT-IR, TGA, elemental analysis, DLS, SEM) whose results are discussed in the Supplementary Information (see experimental section and Figs. S1-S3). The dispersion of graphene sheets was obtained by electrochemically exfoliated method [56]. TEM analysis confirmed the successful exfoliation with flakes displaying lateral dimension of several microns (see Figs. S10 in the Supplementary Information). Noteworthy, graphene sheets were prepared by electrochemical exfoliation and exhibited exceptional electrical conductivity (~600 S cm^{-1}) [65]. The final product (Mo_{132}-DTAB-EEG) was obtained by making use of the non-covalent interactions between long alkyl chains of Mo_{132}-DTAB and the surface of graphene sheets, which represents the first example of such type of Mo_{132} modification. The structure of Mo_{132}-DTAB-EEG (Fig. S4) is held together *via* weak van den Waals interactions, where the Mo_{132}-DTAB acts as spacer, thereby hindering the stacking between adjacent graphene sheets yielding a substantial increase in the materials surface area as portrayed in Fig. 2a. Finally, such highly porous structure of Mo_{132}-DTAB-EEG combines all fundamental characteristics required for being employed as electrode in supercapacitors, ensuring reversible and fast faradaic redox reactions to store the charges.

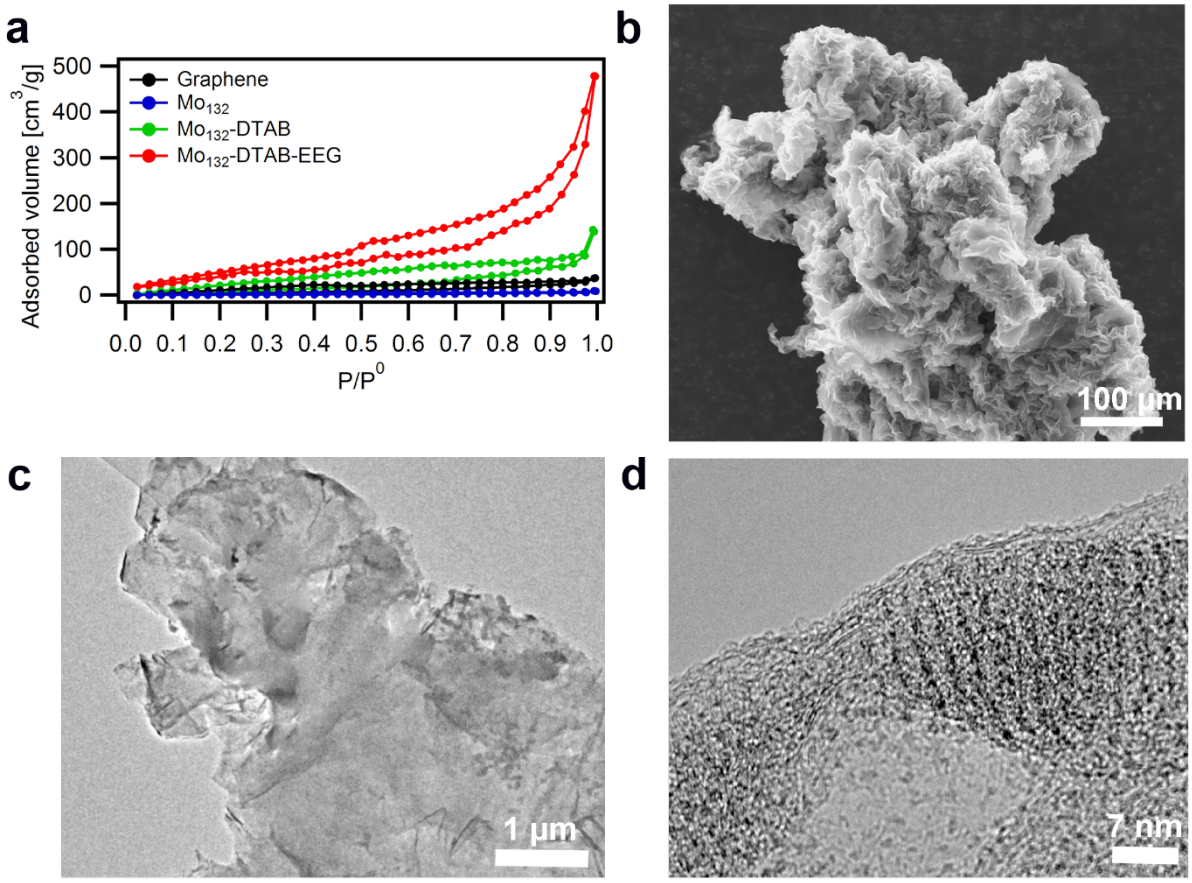

Fig. 2. (a) Nitrogen adsorption–desorption curves for EEG, Mo_{132}, Mo_{132}-DTAB and Mo_{132}-DTAB-EEG samples, respectively. (b) SEM, and (c, d) TEM images of Mo_{132}–DTAB-EEG hybrid material.

Morphological characterization was carried out in order to cast light onto the supramolecular structure resulting from the interactions between Mo_{132}-and the graphene nanosheets. A high specific surface area with a porous structure represents one of the key features required for the development high-performance hybrid electrode materials for energy storage [6, 8]. The Mo_{132}-DTAB-EEG hybrid material exhibits an extremely high Brunauer-Emmett-Teller (BET) surface area (321.91 m^2/g), which is significantly greater than the one of the individual components, the latter amounting to 11.23, 66.35 and 107.94 m^2/g for Mo_{132}, EEG and Mo_{132}-DTAB, respectively (Fig. 2a). N_2 sorption isotherms show a type IV curve with a H2-type hysteresis loop, indicating a mesoporous nature for the majority of pores. The high increase in the active surface of the Mo_{132}-DTAB-EEG sample is attributed to the inclusion of the three-dimensional POM-surfactant nanoparticles which enhances the interlayer distance between the successive graphene sheets. The specific surface area of Mo_{132}-DTAB-EEG is considerably larger than many recently reported carbon/polyoxometalate hybrid materials [49, 50]. For example, Dubal and co-workers obtained a novel hybrid electrode based on $H_3PMo_{12}O_{40}$ Keggin POM anchored onto the reduced graphene oxide (rGO) and reported a maximum BET

surface area of 231.14 m^2/g [41]. The mesoporous nature of Mo_{132}-DTAB-EEG samples was further confirmed by the pore-size distribution analysis displayed in Fig. S8 in the SI indicating an average diameter of pore size calculated at 4.18 and 5.42 nm. Noteworthy, the pore volume of Mo_{132}-DTAB does increase from 0.08 to 0.14 cm^3g^{-1} after functionalization with graphene, which is beneficial during ion insertion/de-insertion into the electrode hybrid material throughout the electrochemical process [66].

Scanning electron microscopy (SEM) and high-resolution transmission electron microscopy (HR-TEM) characterizations of the structure and morphologies of the hybrid materials provide further evidence of the successful dispersion of the Mo_{132}-DTAB into the graphene matrix. X-ray spectroscopy (EDX) measurements (Fig. S4) confirmed the presence of molybdenum, as well as carbon and oxygen in the hybrid structure. The desired homogenous spatial distribution of different elements (C, Mo) in the Mo_{132}-DTAB-EEG hybrid material was monitored by element mapping analysis (Fig. S4). SEM images (Fig. 2b and S5) show that Mo_{132}-DTAB-EEG exhibits a 3D porous and a highly homogenous architecture which is extremely advantageous for boosting the electron transport while maintaining good ionic conductivity. TEM analysis revealed that the surface of the graphene flakes is coated with 3D features which can be ascribed to the Mo_{132}-DTAB superstructures (Fig. 2c and Supplementary Information Fig. S11 for EDS). High-resolution TEM imaging of the flakes surface revealed that many of Mo_{132}-DTAB units are grafted onto the EEG sheets, partially arranging, during TEM observation, with the metal containing clusters (darker regions in Fig. 2d) spaced by a distance compatible with two DTAB units (2.9 nm), as already observed in other POM functionalized materials [67].

Fourier-transform infrared spectroscopy (Fig. S6) revealed that the characteristic bands of Mo_{132} are found in spectra of Mo_{132}-DTAB and Mo_{132}-DTAB-EEG at 721, 798, 864 (Mo-O-Mo) and 979 cm^{-1} (Mo=O) [59]. Such result confirmed the structural integrity of polyoxometalate (Mo_{132}) whose architecture is well retained in the hybrid structures (Mo_{132}-DTAB and Mo_{132}-DTAB-EEG).

The chemical composition and thermal stability of the as-synthesized Mo_{132}-DTAB-EEG was firstly characterized by TGA and XRD, as shown in Figure S7. The Mo_{132}-DTAB-EEG curve (Fig.S7a) displays a weight loss of. ca. 9% between room temperature and 170°C, in agreement with the loss of the solvation water molecules and those located within the cavity of the cluster. Sharper mass percentage drop is monitored around 350°C which can be associated to the

decomposition of the DTAB. XRD powder analysis of Mo_{132}, Mo_{132}-DTAB, DTAB and Mo_{132}-DTAB-EEG systems was performed to confirm the identity of the microcrystalline samples, including their phase purity (Fig. S7b and table S3). In general, flattening of XRD signals that come from POM and DTAB surfactant prove that the material is homogenously dispersed in the EEG matrix. Two distinct broad peaks centered at a 2θ angle of 23.9° and 41.3° appeared, which are characteristic of carbon materials and specifically correspond to the (002) and (001) planes of graphene, respectively [68]. No peak related to the crystal structure of Mo_{132}-DTAB or the sole DTAB is observed, which highlights the absence of Mo_{132}-DTAB superstructures, i.e. agglomerates formed *via* self-assembly of neat Mo_{132}-DTAB clusters. Such evidences demonstrated that Mo_{132}-DTAB clusters are uniformly distributed over graphene nanosheets, thus yielding the desired product [69].

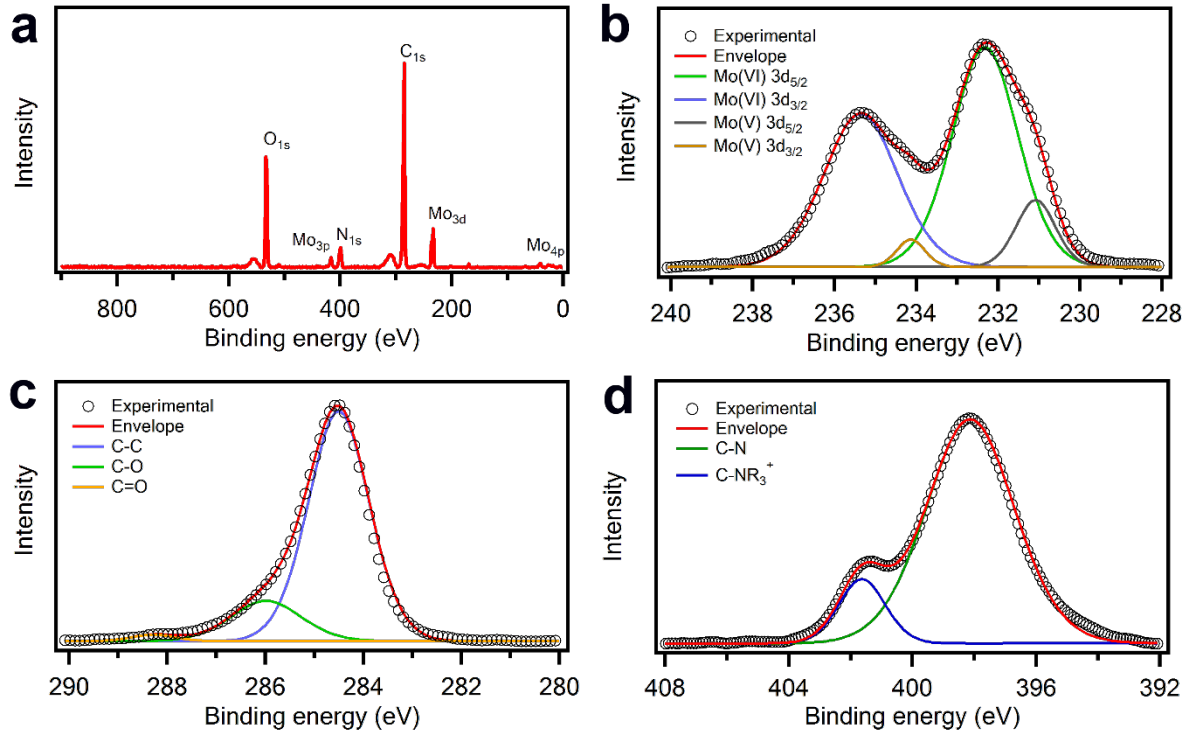

Fig. 3. XPS spectra of Mo_{132}-DTAB-EEG: (a) wide range survey, and high-resolution (b)Mo 3d, (c) C 1s and (d) N 1s.

High resolution X-ray photoelectron spectroscopy (XPS) was performed to gain further information onto the chemical composition in the hybridmaterialcomprising Mo_{132}-DTAB and electrochemically exfoliated graphene (Fig. 3a-d). Figure S9 reveals thatthe pristine Mo_{132} samples displayed a different surface composition with a majority of carbon, oxygen and molybdenum as surface functionalities . For the Mo_{132}-DTAB-EEG modified samples C, O and Mo still appeared as the major surface components(Fig 3a). As shown in Figure 3b, the presence

off our peaks at 231.09, 232.36, 234.28 and 235.42 eV corresponding to $3d_{5/2}$ and $3d_{3/2}$, indicated that the valence state of Mo in the Mo_{132}-DTAB-EEG are +V and +VI [70, 71], and unambiguously confirm the presence of Mo_{132} in the Mo_{132}-DTAB-EEG hybrid material. Moreover, by deconvoluting the high-resolution C 1s spectrum (Fig. 3c), the presence of three carbon-containing functional groups was observed which can be assigned to single bonded carbon-carbon (C-C284.7 eV), epoxy groups (C-O 285.6 eV)and carboxylic moieties (O=CO 288.1 eV) [72]. According toN 1s spectrum (Fig. 3d), two peaks with binding energies of 398.4, and 401.8 eV were identified, which are associated to amine bond (C-N) and quaternary ammonium group ($-NR_3^+$) [73], indicating the successful coating of Mo_{132}-DTAB on the surfaces of EEG sheet. These type of functional groups can efficiently improve the electrical conductivity and induce a pseudocapacitance that should remarkably improve the capacity of supercapcitors. The presence of N species on the graphene surface could generate high pseudocapacitance by mechanisms of acting as electron donor to attract protons or enhancing charge density ofthe space charge layer strengthening the redox reactions of N-containing functional groups [74, 75].

3.2 Electrochemical study

Presented synthetic method makes it possible to exploit the unique redox characteristics of the POM counterpart by simultaneously maximizing its effective surface area upon grafting onto graphene sheets via the DTAB surfactant. Such advantageous combination of different properties can be expected to favor the specific capacitance and thus enhance the electrochemical performance of the supercapacitor when Mo_{132}-DTAB-EEG is employed as electrode material. In order to investigate the electrochemical properties of the Mo_{132}-DTAB-EEG as well as the control sample (Mo_{132}-EEG) as working electrode for supercapacitors, a three-electrode system was assembled by using 1 M H_2SO_4 solution as electrolyte, whereas a platinum plate was employed as a counterelectrode and Ag/AgCl (in saturated KCl) serving as the reference electrode. We decided to exploit an aqueous electrolyte in view of its low toxicity, thus not requiring particular precautions in the device fabrication [38].

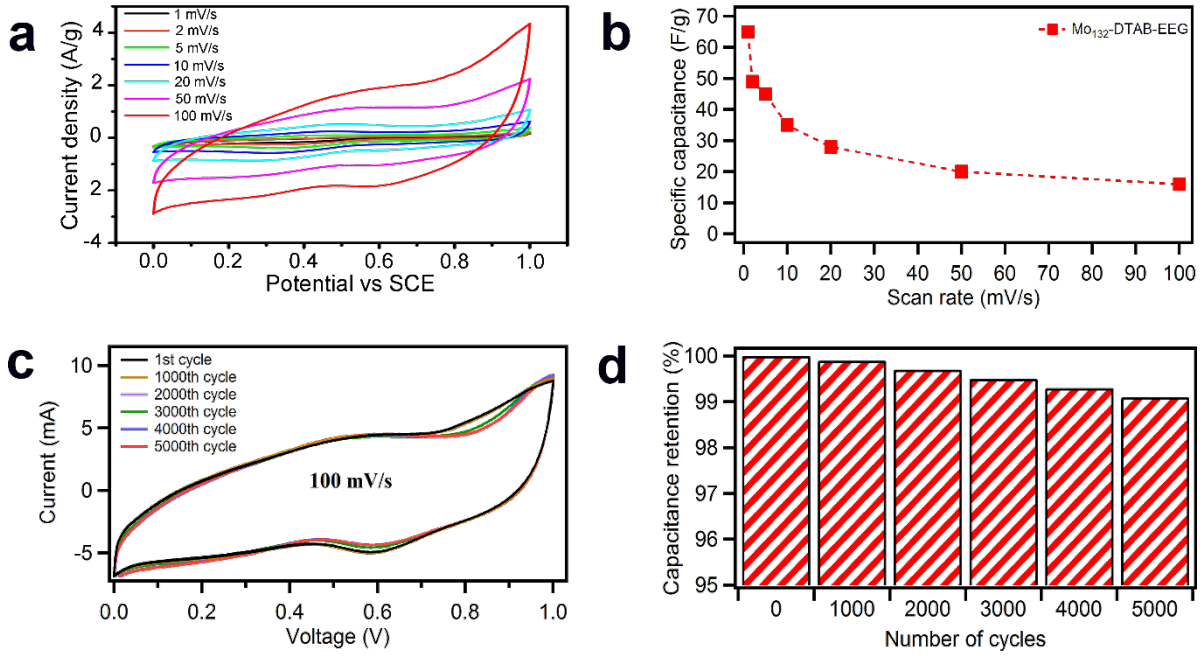

Fig. 4. Electrochemical properties of the Mo_{132}-DTAB-EEG hybrid material: (a) CV curves of Mo_{132}-DTAB-EEG at different scan rates, ranging from 1 mVs^{-1} to 100 mVs^{-1}; (b) Comparison of specific capacitance *vs* scan rate for Mo_{132}-DTAB-EEG; (c-d) Electrochemical cycling stability of Mo_{132}-DTAB-EEG electrode material, CV curves and capacitance retention measured at a scan rate of 100 mVs^{-1}.

The cyclic voltammetry (CV) curves portrayed in Fig. 4a were recorded at different scan rates ranging from 1 mVs^{-1} to 100 mVs^{-1}. Noteworthy, quasi-rectangular shaped CV curves were observed at higher scan rates (20-100 mVs^{-1}) with significant broad redox waves due to the presence of Mo_{132}. Such shape of the CV curves indicates the coexistence of both electrical double layer capacitance provided by electrochemically exfoliated graphene and pseudocapacitance provided by polyoxometalate surface, for the electrochemical behavior of Mo_{132}-DTAB-EEG [46, 76, 77]. The highest value of gravimetric specific capacitance reached (65 Fg^{-1}) at scan rate of 1 mV s^{-1} (Fig. 4b), is comparable with previously reported graphene-POM hybrid materials [41]. It is important to note that high molecular mass of Keplerate POM will always limit the gravimetric capacity, therefore surface and volumetric capacities are more practical parameters to compare (93 $mFcm^{-2}$ and 93 Fcm^{-3} respectively for Mo_{132}-DTAB-EEG). Moreover, significant increase in those values was noted in comparison to the sole graphene G from different reduction methods (0.51-2.3 $mFcm^{-2}$ and 3.1-17.9 Fcm^{-2}) [78]. Such an increase can be attributed to the enhanced surface area of the Keplerate based composite and redox activity of POM cluster. Moreover, the CV curves displayed in Fig. 4c confirm that cycling does not cause significant degradation of the electrochemical performance. Therefore, the presented system exhibits effective energy storage performance with high durability

outperforming other polyoxometalate-based supercapacitors [79]. The detailed cycling performance of Mo_{132}-DTAB-EEG at a scan rate of 100 mVs^{-1} is displayed in Fig. 4d. Noteworthy, there is no obvious capacitance drop (~ 99 % capacitance retention) up to 5000 cycles proving excellent electrochemical stability of the obtained polyoxometalate/graphene hybrid material. As expected, the electrochemical cycling stability test showed that after several cycles the hysteresis loop changes its shape drastically, which unambiguously indicates the instability of the Mo_{132}-EEG system. Moreover, the value of specific capacitance was ca. 4 times lower comparison to Mo_{132}-DTAB-EEG (see SI table S1) and may be related to other class of supercapacitor hybrid materials (Table S2). This material is particularly appealing for supercapacitor applications since it provides a platform that displays unexpectedly high electrochemical stability, irrespectively of the big structural nature of the Mo_{132} POM. Mechanism of action that explains observed electrochemical results may be ascribed to the synergic effect of both EDL and the pseudocapacitance components. The electric double-layer mechanism between ions and the negatively charged electrode is primarily a result of the EEG, which exhibits an overall high electrical conductivity. The pseudocapacitive contribution is a result of the reversible surface redox reactions between the electrolyte and the electrode, stemming from the redox characteristics of the Mo_{132} POM. Noteworthy, the presence of DTAB surfactants allowed to integrate both electroactive counterparts, thus providing a hybrid material with exceptional stability and without electrochemical drawbacks of the individual counterparts (POM – low electronic conductivity; EEG – limited charge storage capability)."

4. Conclusions

In summary, we have demonstrated for the first time that the Keplerate type polyoxometalate Mo_{132} can be used to tailor novel Mo_{132}-DTAB-EEG hybrids as electrode materials for supercapacitors. The hybrid material was generated by exploiting of a simple two-step synthetic methodology which relies on the use of DTAB to form the surfactant encapsulated cluster Mo_{132}-DTAB, which, *via* van der Waals interaction with the electrochemically exfoliated graphene, forms a Mo_{132}-DTAB-EEG composite displaying synergically increased porosity and thus enhanced supercapacitive performance. The novel porous material exhibits significantly higher specific, volumetric and surface capacitance parameters compared to the non-functionalized graphene in the acidic aqueous solution (1M H_2SO_4), 0-1 V potential window followed by excellent electrochemical cycling stability (99% of specific capacitance retained) after 5000 charge/discharge cycles. This work enriches the current family of POM-based carbon

composites and provides a solid evidence that polyoxometalates of other chemical composition than Keggin or Wells-Dawson. The greater degree of functionalization that can be achieved when using Keplerate type polyoxometalate enables better tuning of a variety of physico-chemical properties of the hybrid system towards the emergence of a new generation of high performing multifunctional supercapacitors possessing enhanced stability.

Acknowledgements

This work was supported by the National Science Center (Grant No.2015/18/E/ST5/00188, Grant No. 2016/21/B/ST5/00175 and Grant No.2017/27/N/ST5/00173) and the European Commission through the Graphene Flagship Core 2 project (GA-785219), the Agence Nationale de la Recherche through the Labex project CSC (ANR-10-LABX-0026 CSC) within the Investissement d'Avenir program (ANR-10-120 IDEX-0002-02), and the International Center for Frontier Research in Chemistry (icFRC). D. P. acknowledges the support from the Embassy of France in Poland in the form of a scholarship at the Institut de Science et d'Ingenierie Supramoleculaires, University of Strasbourg.

Competing financial interests

The authors declare no competing financial interests.

Appendix A. Supporting Information

Supplementary data associated with this article can be found in the online version at

References

[1] A.C. Ferrari, F. Bonaccorso, V. Fal'ko, K.S. Novoselov, S. Roche, P. Bøggild, S. Borini, F.H.L. Koppens, V. Palermo, N. Pugno, J.A. Garrido, R. Sordan, A. Bianco, L. Ballerini, M. Prato, E. Lidorikis, J. Kivioja, C. Marinelli, T. Ryhänen, A. Morpurgo, J.N. Coleman, V. Nicolosi, L. Colombo, A. Fert, M. Garcia-Hernandez, A. Bachtold, G.F. Schneider, F. Guinea, C. Dekker, M. Barbone, Z. Sun, C. Galiotis, A.N. Grigorenko, G. Konstantatos, A. Kis, M. Katsnelson, L. Vandersypen, A. Loiseau, V. Morandi, D. Neumaier, E. Treossi, V. Pellegrini, M. Polini, A. Tredicucci, G.M. Williams, B. Hee Hong, J.H. Ahn, J. Min Kim, H. Zirath, B.J. Van Wees, H. Van Der Zant, L. Occhipinti, A. Di Matteo, I.A. Kinloch, T. Seyller, E. Quesnel, X. Feng, K. Teo, N. Rupesinghe, P. Hakonen, S.R.T. Neil, Q. Tannock, T. Löfwander, J. Kinaret, Nanoscale, 7 (2015) 4598-4810.
[2] F. Bonaccorso, L. Colombo, G. Yu, M. Stoller, V. Tozzini, A.C. Ferrari, R.S. Ruoff, V. Pellegrini, Science, 347 (2015) 1246501.
[3] P. Simon, Y. Gogotsi, Nat. Mater., 7 (2008) 845.
[4] Z. Lin, E. Goikolea, A. Balducci, K. Naoi, P.L. Taberna, M. Salanne, G. Yushin, P. Simon, Mater. Today, 21 (2018) 419-436.

[5] J. Vatamanu, O. Borodin, M. Olguin, G. Yushin, D. Bedrov, J. Mater. Chem. A, 5 (2017) 21049-21076.
[6] M. Winter, R.J. Brodd, Chem. Rev., 104 (2004) 4245-4270.
[7] Y. Zhang, H. Feng, X. Wu, L. Wang, A. Zhang, T. Xia, H. Dong, X. Li, L. Zhang, Int. J. Hydrogen Energy, 34 (2009) 4889-4899.
[8] F. Wang, X. Wu, X. Yuan, Z. Liu, Y. Zhang, L. Fu, Y. Zhu, Q. Zhou, Y. Wu, W. Huang, Chem. Soc. Rev., 46 (2017) 6816-6854.
[9] D.P. Dubal, N.R. Chodankar, D.-H. Kim, P. Gomez-Romero, Chem. Soc. Rev., 47 (2018) 2065-2129.
[10] D.P. Dubal, O. Ayyad, V. Ruiz, P. Gómez-Romero, Chem. Soc. Rev., 44 (2015) 1777-1790.
[11] X. Huang, X. Qi, F. Boey, H. Zhang, Chem. Soc. Rev., 41 (2012) 666-686.
[12] E. Frackowiak, Q. Abbas, F. Béguin, J. Energy Chem., 22 (2013) 226-240.
[13] J. Zhang, M. Terrones, C.R. Park, R. Mukherjee, M. Monthioux, N. Koratkar, Y.S. Kim, R. Hurt, E. Frackowiak, T. Enoki, Y. Chen, Y. Chen, A. Bianco, Carbon, 98 (2016) 708-732.
[14] S. Kumar, M. Nehra, D. Kedia, N. Dilbaghi, K. Tankeshwar, K.-H. Kim, Prog. Energy Combust. Sci., 64 (2018) 219-253.
[15] R. Kumar, E. Joanni, R.K. Singh, D.P. Singh, S.A. Moshkalev, Prog. Energy Combust. Sci., 67 (2018) 115-157.
[16] E. Quesnel, F. Roux, F. Emieux, P. Faucherand, E. Kymakis, G. Volonakis, F. Giustino, B. Martín-García, I. Moreels, S.A. Gürsel, A.B. Yurtcan, V. Di Noto, A. Talyzin, I. Baburin, D. Tranca, G. Seifert, L. Crema, G. Speranza, V. Tozzini, P. Bondavalli, G. Pognon, C. Botas, D. Carriazo, G. Singh, T. Rojo, G. Kim, W. Yu, C.P. Grey, V. Pellegrini, 2D Mater., 2 (2015).
[17] M. Sevilla, G.A. Ferrero, A.B. Fuertes, Energy Storage Mater., 5 (2016) 33-42.
[18] B. Zhao, D. Chen, X. Xiong, B. Song, R. Hu, Q. Zhang, B.H. Rainwater, G.H. Waller, D. Zhen, Y. Ding, Y. Chen, C. Qu, D. Dang, C.-P. Wong, M. Liu, Energy Storage Mater., 7 (2017) 32-39.
[19] X. Wang, S.-X. Zhao, L. Dong, Q.-L. Lu, J. Zhu, C.-W. Nan, Energy Storage Mater., 6 (2017) 180-187.
[20] T. Brousse, D. Bélanger, J.W. Long, J. Electrochem. Soc., 162 (2015) A5185-A5189.
[21] D.P. Dubal, N.R. Chodankar, P. Gomez-Romero, D.-H. Kim, 4 - Fundamentals of Binary Metal Oxide–Based Supercapacitors, in: D.P. Dubal, P. Gomez-Romero (Eds.) Metal Oxides in Supercapacitors, Elsevier, 2017, pp. 79-98.
[22] M.-R. Gao, Y.-F. Xu, J. Jiang, S.-H. Yu, Chem. Soc. Rev., 42 (2013) 2986-3017.
[23] A. Eftekhari, L. Li, Y. Yang, J. Power Sources, 347 (2017) 86-107.
[24] Y. Huang, H. Li, Z. Wang, M. Zhu, Z. Pei, Q. Xue, Y. Huang, C. Zhi, Nano Energy, 22 (2016) 422-438.
[25] B.D. Boruah, A. Misra, Energy Storage Mater., 5 (2016) 103-110.
[26] L. De-Liang, T. Ryo, C. Leroy, Angew. Chem. Int. Ed., 49 (2010) 1736-1758.
[27] M. Ammam, J. Mater. Chem. A, 1 (2013) 6291-6312.
[28] M. Genovese, K. Lian, 6 - Polyoxometalates: Molecular Metal Oxide Clusters for Supercapacitors, in: D.P. Dubal, P. Gomez-Romero (Eds.) Metal Oxides in Supercapacitors, Elsevier, 2017, pp. 133-164.
[29] U. Tadaharu, ChemElectroChem, 5 (2018) 823-838.
[30] A. Yamada, J.B. Goodenough, J. Electrochem. Soc., 145 (1998) 737-743.
[31] A.K. Cuentas-Gallegos, M. Lira-Cantú, N. Casañ-Pastor, P. Gómez-Romero, Adv. Funct. Mater., 15 (2005) 1125-1133.
[32] T. Akter, K. Hu, K. Lian, Electrochim. Acta, 56 (2011) 4966-4971.
[33] M. Genovese, K. Lian, Electrochem. Commun., 43 (2014) 60-62.
[34] V. Prabhakaran, B.L. Mehdi, J.J. Ditto, M.H. Engelhard, B. Wang, K.D.D. Gunaratne, D.C. Johnson, N.D. Browning, G.E. Johnson, J. Laskin, Nature Communications, 7 (2016) 11399.

[35] M. Skunik, M. Chojak, I.A. Rutkowska, P.J. Kulesza, Electrochimica Acta, 53 (2008) 3862-3869.
[36] M. Sosnowska, M. Goral-Kurbiel, M. Skunik-Nuckowska, R. Jurczakowski, P.J. Kulesza, Journal of Solid State Electrochemistry, 17 (2013) 1631-1640.
[37] H.-Y. Chen, R. Al-Oweini, J. Friedl, C.Y. Lee, L. Li, U. Kortz, U. Stimming, M. Srinivasan, Nanoscale, 7 (2015) 7934-7941.
[38] J. Suárez-Guevara, V. Ruiz, P. Gomez-Romero, J. Mater. Chem. A, 2 (2014) 1014-1021.
[39] C. Hu, E. Zhao, N. Nitta, A. Magasinski, G. Berdichevsky, G. Yushin, Journal of Power Sources, 326 (2016) 569-574.
[40] V. Ruiz, J. Suárez-Guevara, P. Gomez-Romero, Electrochemistry Communications, 24 (2012) 35-38.
[41] D.P. Dubal, J. Suarez-Guevara, D. Tonti, E. Enciso, P. Gomez-Romero, J. Mater. Chem. A, 3 (2015) 23483-23492.
[42] J. Qin, F. Zhou, H. Xiao, R. Ren, Z.-S. Wu, Science China Materials, 61 (2018) 233-242.
[43] J. Suárez-Guevara, V. Ruiz, P. Gómez-Romero, Physical Chemistry Chemical Physics, 16 (2014) 20411-20414.
[44] Y. MinHo, C.B. Gill, J.S. Chul, H. Young-Kyu, H.Y. Suk, L.S. Bok, Advanced Functional Materials, 24 (2014) 7301-7309.
[45] D.P. Dubal, B. Nagar, J. Suarez-Guevara, D. Tonti, E. Enciso, P. Palomino, P. Gomez-Romero, Mater. Today Energy, 5 (2017) 58-65.
[46] D.D. P., C.N. R., V. Ajayan, K. Do-Heyoung, G.-R. Pedro, ChemSusChem, 10 (2017) 2742-2750.
[47] P. Dubal Deepak, D. Rueda-Garcia, C. Marchante, R. Benages, P. Gomez-Romero, Chem. Rec., 18 (2018) 1076-1084.
[48] M. Genovese, K. Lian, Curr. Opin. Solid State Mater. Sci., 19 (2015) 126-137.
[49] Y. Ji, L. Huang, J. Hu, C. Streb, Y.-F. Song, Energy Environ. Sci., 8 (2015) 776-789.
[50] M. Zhang, T. Wei, A.M. Zhang, S.-L. Li, F.-C. Shen, L.-Z. Dong, D.-S. Li, Y.-Q. Lan, ACS Omega, 2 (2017) 5684-5690.
[51] F.M. Toma, A. Sartorel, M. Iurlo, M. Carraro, P. Parisse, C. MacCato, S. Rapino, B.R. Gonzalez, H. Amenitsch, T. Da Ros, L. Casalis, A. Goldoni, M. Marcaccio, G. Scorrano, G. Scoles, F. Paolucci, M. Prato, M. Bonchio, Nat. Chem., 2 (2010) 826-831.
[52] A. Nisar, X. Wang, Dalton Trans., 41 (2012) 9832-9845.
[53] Jiangwei Zhang, Yichao Huang, Y. Wei, POM-based chiral hybrids via organically covalent modification of achiral presursors, in: Laurent Ruhlmann, D. Schaming (Eds.) Trends in Polyoxometalates Research, Nova Science Publishers, New York, 2015, pp. 37-71.
[54] P. Yin, D. Li, T. Liu, Chem. Soc. Rev., 41 (2012) 7368-7383.
[55] L. Zhang, H. Li, L. Wu, Soft Matter, 10 (2014) 6791-6797.
[56] M. Eredia, S. Bertolazzi, T. Leydecker, M. El Garah, I. Janica, G. Melinte, O. Ersen, A. Ciesielski, P. Samorì, J. Phys. Chem. Lett., 8 (2017) 3347-3355.
[57] M. Achim, K. Erich, B. Hartmut, S. Marc, P. Frank, Angew. Chem. Int. Ed., 37 (1998) 3359-3363.
[58] S. Floquet, E. Terazzi, A. Hijazi, L. Guenee, C. Piguet, E. Cadot, New J. Chem., 36 (2012) 865-868.
[59] H. Li, Y. Yang, Y. Wang, C. Wang, W. Li, L. Wu, Soft Matter, 7 (2011) 2668-2673.
[60] A. Müller, P. Gouzerh, Chem. Soc. Rev., 41 (2012) 7431-7463.
[61] A. Rezaeifard, R. Haddad, M. Jafarpour, M. Hakimi, ACS Sustainable Chem. Eng., 2 (2014) 942-950.
[62] I. Baroudi, C. Simonnet-Jégat, C. Roch-Marchal, N. Leclerc-Laronze, C. Livage, C. Martineau, C. Gervais, E. Cadot, F. Carn, B. Fayolle, N. Steunou, Chem. Mater., 27 (2015) 1452-1464.
[63] S. Xu, Y. Wang, Y. Zhao, W. Chen, J. Wang, L. He, Z. Su, E. Wang, Z. Kang, J. Mater. Chem. A, 4 (2016) 14025-14032.

[64] D. Volkmer, A. Du Chesne, D.G. Kurth, H. Schnablegger, P. Lehmann, M.J. Koop, A. Müller, J. Am. Chem. Soc., 122 (2000) 1995-1998.
[65] K. Parvez, R. Li, S.R. Puniredd, Y. Hernandez, F. Hinkel, S. Wang, X. Feng, K. Müllen, ACS Nano, 7 (2013) 3598-3606.
[66] M. Salanne, B. Rotenberg, K. Naoi, K. Kaneko, P.L. Taberna, C.P. Grey, B. Dunn, P. Simon, Nat. Energy, 1 (2016) 16070.
[67] S. Floquet, E. Terazzi, A. Hijazi, L. Guénée, C. Piguet, E. Cadot, New J Chem, 36 (2012) 865-868.
[68] H. Kim, K.-Y. Park, J. Hong, K. Kang, Sci. Rep., 4 (2014) 5278.
[69] Y.-H. Ding, J. Peng, H.-Y. Lu, Y. Yuan, S.-U. Khan, RSC Adv., 6 (2016) 81085-81091.
[70] Y. Zhu, Z. Yuan, W. Cui, Z. Wu, Q. Sun, S. Wang, Z. Kang, B. Sun, J. Mater. Chem. A, 2 (2014) 1436-1442.
[71] D. Anne, C. Jean-Daniel, M. Pierre, M. Jérôme, S. Francis, K. Bineta, H.L.R. Brudna, M. Frédéric, N. Louis, Chem – Eur. J., 15 (2009) 733-741.
[72] T. Zhu, J. Zhou, Z. Li, S. Li, W. Si, S. Zhuo, J. Mater. Chem. A, 2 (2014) 12545-12551.
[73] Q. Hao, X. Xia, W. Lei, W. Wang, J. Qiu, Carbon, 81 (2015) 552-563.
[74] F. Su, C.K. Poh, J.S. Chen, G. Xu, D. Wang, Q. Li, J. Lin, X.W. Lou, Energy Environ. Sci., 4 (2011) 717-724.
[75] X. Yang, D. Wu, X. Chen, R. Fu, J. Phys. Chem. C, 114 (2010) 8581-8586.
[76] K. Kume, N. Kawasaki, H. Wang, T. Yamada, H. Yoshikawa, K. Awaga, Journal of Materials Chemistry A, 2 (2014) 3801-3807.
[77] R. Li, C. He, L. Cheng, G. Lin, G. Wang, D. Shi, R.K.-Y. Li, Y. Yang, Composites Part B: Engineering, 121 (2017) 75-82.
[78] L. Zhaoyang, W. Zhong-Shuai, Y. Sheng, D. Renhao, F. Xinliang, M. Klaus, Adv. Mater., 28 (2016) 2217-2222.
[79] A.K. Cuentas-Gallegos, R. Martínez-Rosales, M. Baibarac, P. Gómez-Romero, M.E. Rincón, Electrochemistry Communications, 9 (2007) 2088-2092.